Politecnico di Milano

Scuola di Ingegneria Industriale e dell'Informazione

Course of numerical analysis for partial differential equations

Metal Artifact Reduction

Rafael Vital Rodrigues

Matriculation 815993

Academic year 2014−2015

Contents

Chapter 1

Theory

1.1 Image

In computer science, a 2d-image is defined by a function f(x,y) where (x,y) are spacial coordinate of a plane and the amplitude represent the gray level of the point.

There are many tools to work with the image. The most common is the filters. A filter is a function defined on the plane (x,y), in such way, its 2D-convolution with a image is able to extract some feature of this image. Two traditional filter are the high-pass filter, which emphasizes the lines and curve of the image, and the low-pass filter, which blur the image reducing the noise of the image.

Another tools is the transformation. The transformation take a function f, thus the image, and apply a operation that change the domain and consequentially the amplitude of the image. The goal is evidence something which was difficult to see on the original domain.

One of the most famous transformation is the Fourier transform, defined by:

$$F(m,n) = \int_{-\infty}^{\infty} \int_{-\infty}^{\infty} f(x,y) \mathrm{e}^{-2\pi \mathrm{i}(mx+ny)} \mathrm{d}x\mathrm{d}y \qquad (1.1)$$

Further, the Radon transform is well-know transform which has a important role in tomography.

1.2 Radon transform

The Radon transform maps a function f(x,y) into the set of all its line integrals:

$$(Rf)(l) = \int_l f(x,y)ds$$

4

Where we can parameterize l as a affine function in the cartesian coordinate.

$$R(p,q) = \int_{-\infty}^{\infty} f(x, px+q)\mathrm{d}x.$$

Sometimes is useful read the Radon transform in the polar coordinate, so:

$$R(\theta, x') = \int_{-\infty}^{\infty} \int_{-\infty}^{\infty} f(x', y')\mathrm{d}x'\mathrm{d}y'$$
$$= \int_{-\infty}^{\infty} \int_{-\infty}^{\infty} f(x\cos\theta + y\sin\theta, -x\sin\theta + y\cos\theta)\mathrm{d}x\mathrm{d}y \qquad (1.2)$$

Where,

$$x' = x\cos\theta + y\sin\theta$$
$$y' = -x\sin\theta + y\cos\theta$$
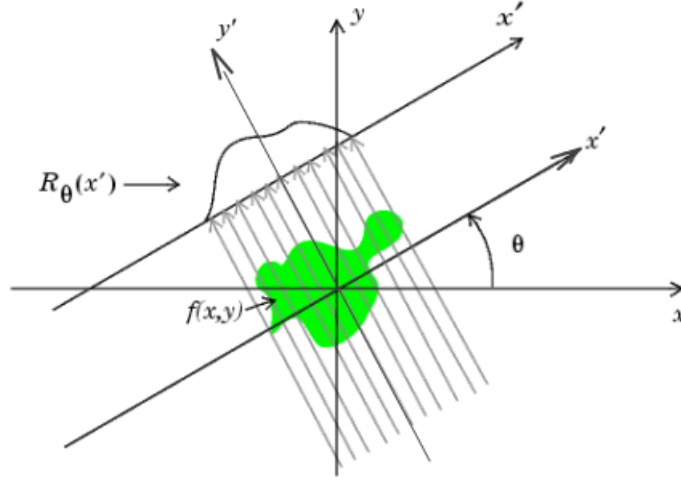
Figure 1.1: Referential system of radon transform

So, we can transform a image that is in Cartesian domain to another image in radon domain using the equation (1.2), the image in the radon domain is called sinogram. The opposite, from sinogram obtain a Cartesian image can't be done directly.

However exist another way to accomplish this task.

The inversion is done through a relationship between Fourier Transform of Radon Transform.

$$P(\theta, k') = \int_{-\infty}^{\infty} R(\theta, x')\mathrm{e}^{-2\pi\mathrm{i}k'x'}\mathrm{d}x'$$

Using (1.2),

$$P(\theta, k') = \int_{-\infty}^{\infty} \left(\int_{-\infty}^{\infty} f(x', y') \mathrm{d}y' \right) \mathrm{e}^{-2\pi \mathrm{i} k' x'} \mathrm{d}x'$$

$$P(\theta, k') = \int_{-\infty}^{\infty} \int_{-\infty}^{\infty} f(x', y') \mathrm{e}^{-2\pi \mathrm{i} k'(x \cos \theta + y \sin \theta)} \mathrm{d}x' \mathrm{d}y'$$

$$P(\theta, k') = F(k' \cos \theta, k' \sin \theta) \tag{1.3}$$

The equation (1.3), known by theorem of the central section, says that the Fourier transform of a projection $P(\theta, k')$, is equal to the Fourier transform of $f(x, y)$ calculated along the strait line described by the angle θ with respect to k on the plane (k, l).

So, if we take the Radon transform of a image F, put it on the polar coordinate, do its Fourier transform, return it to the Cartesian coordinate, and do its inverse Fourier transform, we retrieve the image F.

In theory this method work, but in practice we can't do it, because we have a finite number of projection, i.e, we have projection only for a few number of discrete angles. A ingenious procedure to resolve it, would be interpolate the missing data, although this method adds high frequency error on the reconstruct image.

Since is not recommended to do the restoration using Fourier transform, were created a alternative method which is based on the theorem of the central section.

Starting from the Fourier transform of the image F and putting it on polar coordinate, we obtain $F(\theta, k')$. Thus, to get back the image f, the inverse Fourier transformed can be written like this.

$$f(x, y) = \int_{-\infty}^{\infty} \int_{-\infty}^{\infty} F(m, n) \mathrm{e}^{2\pi \mathrm{i}(mx + ny)} \mathrm{d}m \mathrm{d}n$$

$$f(x, y) = \int_{0}^{2\pi} \int_{0}^{\infty} F(k' \cos \theta, k' \sin \theta) \mathrm{e}^{2\pi \mathrm{i} k'(x \cos \theta + y \sin \theta)} k' \mathrm{d}k' \mathrm{d}\theta$$

Where,

$$m = k' \cos \theta$$

$$l = k' \sin \theta$$

So, using the central section theorem (1.3), we obtain

$$f(x, y) = \int_{0}^{2\pi} \int_{0}^{\infty} P(\theta, k') \mathrm{e}^{2\pi \mathrm{i} k'(x \cos \theta + y \sin \theta)} k' \mathrm{d}k' \mathrm{d}\theta,$$

which can be manipulated, applying the symmetry property, arriving to

$$f(x,y) = \int_0^\pi \int_{-\infty}^\infty P(\theta, k') \mathrm{e}^{2\pi \mathrm{i} k'(x\cos\theta + y\sin\theta)} |k'| \mathrm{d}k' \mathrm{d}\theta$$

$$= \int_0^\pi \int_{-\infty}^\infty P(\theta, k') \mathrm{e}^{2\pi \mathrm{i} k' x'} |k'| \mathrm{d}k' \mathrm{d}\theta.$$

Thus,

$$f(x,y) = \int_0^\pi C(\theta, x) \mathrm{d}\theta. \tag{1.4}$$

Where,

$$C(\theta, x) = \int_{-\infty}^\infty P(\theta, k') |k'| \mathrm{e}^{2\pi \mathrm{i} k' x'} \mathrm{d}k'$$

and this can be interpreted as a convolution, because

$$C(\theta, x) = \mathrm{F}^{-1}(\mathrm{F}(R)\mathrm{F}(B))$$

$$B(k') = \begin{cases} |k'| & k' < \frac{1}{2\Delta x'} \\ 0 & \text{otherwise} \end{cases}$$

$B(k')$ is defined in this way because we need to take in consideration the Shannon-Nyquist theorem, that specify the maximum possible frequency with respect to the number of samples, so $B(k')$ is responsible for the term $B(k')$ and to limit the frequency.

Therefore,

$$C(\theta, x) = R(\theta, x') * B(x') \tag{1.5}$$

Finally, the equation (1.4) show how restore image through the convolution obtained in (1.5).

This method is called Filtered Back Projection.

1.3 The Computed Tomography

Computed tomography(CT) or computerized axial tomography (CAT) is an X-ray procedure that combines many X-ray's measures to generate sectional view of a object. The computed tomography has a great number of applications. In medicine is used to do noninvasive diagnostics, on the homeland security, to identify illegal material in airports, on geology, to identify oil and to create earth imaging.

The measure evaluates the difference of the X-ray's intensity between the pair transmitter/receiver. The attenuation occurs when the x-ray pass by the object, the bigger is the object, higher will be the mitigation, furthermore each object has a different attenuation coefficient, for instance the attenuation caused by water is smaller than that caused by metal.

One time we have the attenuation's measures of different angles and positions, we can create the inverse problem such that the solution is the sectional view of the object.

But which measures (angles and positions) are necessary to define the problem and how resolve it?

To answer this question, we need specify what the attenuation means in a mathematical term. It is given by the beer's law.

$$\frac{\mathrm{d}I}{\mathrm{d}x} = -\mu(x)\Delta x$$
$$I_1 = I_0 e^{-\int_L \mu(x)\mathrm{d}x}$$
$$\int_L \mu(x)\mathrm{d}x = log\frac{I_0}{I_1} \tag{1.6}$$

Is easy to see that the beer's law is very similar to the formulation of the Radon transform. Furthermore is known that the filtered backprojection method retrieve the original image, starting from the data in Radon domain.

Knowing this two things we are able to define and resolve the inverse problem, the solution is based on the application of FBP on the X-ray's measures that represent the sectional image on the Radon domain. The simple way to do it is using parallel beam (1.2), in such way, we can take all projection generated by these beans in all directions to get the Radon transform of the sectional.

So, the tomography is based in two step: The first is responsible for acquire the "Radon transform" from the object's slice using the beer's law; the second establish a image through filtered backprojection of the acquired data.
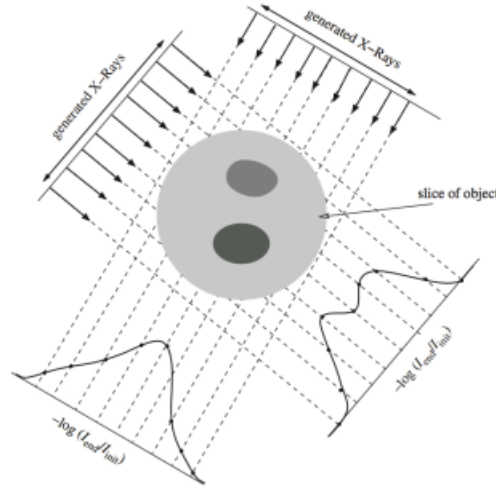
Figure 1.2: Parallel Beam

1.3.1 Problems

Although the tomography techniques work well exist a lot of problems in this procedure.

The first class of problems is due to the measures of the X-ray's intensity. This measures are susceptible to different types of noise: a common noise that all physical sensor have, noise caused by the scatter effect, where some photons don't go in straight line but deflects on a object, so the pair intensity transmitted/received not always refers to the same photons, and noise caused by the environment.

The second class of problems is related to how the projections are done, i.e, if exist a insufficient number of lines in a projection, or a insufficient number of projections or a projection is corrupted by dense object, that don't allow the x-ray pass it.

The second class of problems is more common in medical tomography, because we don't want expose the patient to a unnecessary radiation doses. In this project we will focus on the error caused by a metallic object inside a patience.

1.4 Metal Artifact Reduction

When we do a CT, if there is a object with a great electrical density, the final image is corrupted. This happens because these object obstruct the way of photons, so only a small number of photons, that have high energy, arrive on the sensors, then the measure is inconsistent.

These objects are in general metals, like prosthesis and peacemaker. So we call this phenomenons of Metal Artifact.

Metal Artifact Reduction is a process where the goal is reduce the error caused by the metal. There is a lot of different ways to resolve this problem. One way is interpret all measures that was altered due to the metal as lack of date. So we can use the others date to estimate them.

A large number of algorithms do the estimate through interpolation. But how interpolate? How identify the corrupt and incorrupt date? Due to the nature of CT is mandatory interpret the image not only on the 'Cartesian domain' but on the 'Radon domain' too. The 'Radon domain' is a good tool because each point represent uniquely a measure. So if we know which measures are incorrect, we can discovery, on the Radon domain, exactly which point are corrupted or not. Knowing these points we are promptly to apply any interpolation algorithm.

One way to identify the incorrect measure is discovering where is the metal on the Cartesian domain and then apply the Radon transform on these points. See a example on the figure (1.3).
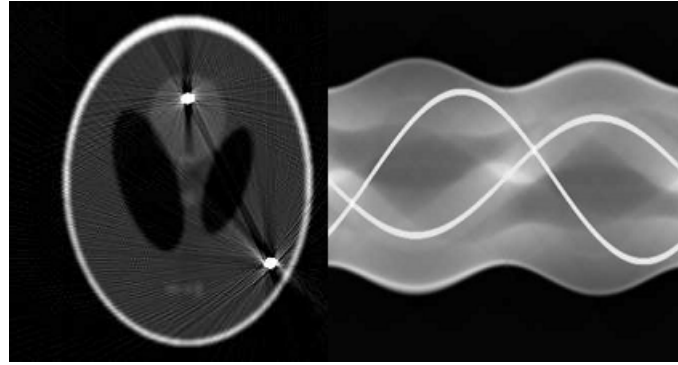

Figure 1.3: The metallic part is the pixel with greater white intensity: On the left the image on Cartesian coordinate, on the right the sinogram (Radon Transform)

After identify which measures is incorrect and consequently which points on 'Radon domain' is corrupted, we can interpolate the date on the 'Radon domain' and then transform the result to the 'Cartesian domain', so we

obtain the recovered image.

1.4.1 Interpolation Methods

There is a lot different ways to interpolate a data: linear interpolation, polynomial interpolation, using finite elements, minimizing a variation function,respecting a partial differential equation and so on. On the next topics we will do a brief explain on two methods, linear interpolation and the method of Bertalmio at el, which relies on the solution of a partial difference equation.

1.4.2 Linear

This method consist in interpolate all the project respect to θ. In other words, for each θ we have a segment $X_d(\cdot, \theta)$ composed by cleaned and corrupted interval. The interval where the date is corrupted is restored using linear functions that connects its extremes, that are reliable data.
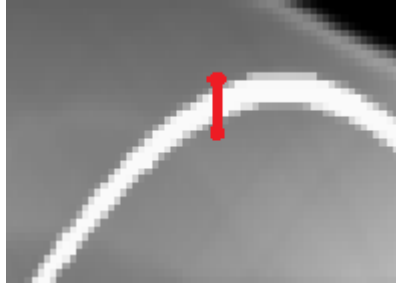

Figure 1.4: Linear Interpolation, the red line on the sinogam represent the changed pixel and the interpolation extremes

1.4.3 Method of Bertalmio at el

This approach is based on interpreter the Radon transform as a image and then apply the techniques of image inpainting. Image inpainting is the process of reconstructing lost or deteriorated parts of images.

The Bertalmio at el. method is inspired on the work of art restorer. The main point is that the structure surrounding the deteriorated area are continued inside the gap. So the contour lines are drawn as extensions of the contour lines that touch the edge of the domain.

Furthermore, the properties of the contour lines inside the deteriorated domain, like color and smoothness, is determined by the properties that this contour line have on the edge of the domain.

In mathematics terms, the contour lines is represented by $u(x; y) = c$, where u is the grey intensity. Then the direction of the contour line is $\nabla^\perp u$ and the smoothness is defined by Δu.

The Laplacian is a good estimate of smoothness because it has a large value when the variation is high and a small value when the region is regular. Furthermore, the laplacian is related to the border in the images. So, when we propagate the laplacian we are prolonging the borders.

Therefore, we need propagate the Δu over $\nabla^\perp u$ until arrive in a stationary condition.

The equations that describe the propagation is

$$u_t = \nabla u \cdot \nabla \Delta u \tag{1.7}$$

and is possible add a diffusion term ($\nu \nabla \cdot (g(|\nabla u|) \nabla u)$) in order to obtain a smother image.

The stationary condition is reached when u^* (the solution) satisfy

$$\nabla^\perp u^* \cdot \nabla \Delta u^* = 0,$$

because in this condition the contour lines of u^* and the Δu^* are parallels. So, there aren't anything more to propagate.

The equation (1.7) says how the image behave inside of the deteriorated domain. Obviously, on the border of the domain u^* need be equal to the imagine outside of the domain. Thus, The edge conditions can be translate by

$$\begin{cases} u^* = u & \partial D \\ \nabla^\perp u^* = \nabla^\perp u & \partial D \end{cases}$$

Analogy between fluid and image

Consider the Navier Stoker Equations for a incompressible viscous fluid.

$$\begin{cases} v_t + v \cdot \nabla v - \nu \Delta v + \nabla p = 0 & D \\ \nabla v = 0 & D \end{cases}$$

Is possible prove that, in the bidimensinal case of incompressible constrains, exit a flow function Ψ in such way $v = \nabla \Psi$.

Further, we can describe the Navier Stoker Equation with the vorticity ω instead of use v.

So,

$$\omega_t + v \cdot \nabla \omega - \nu \Delta \omega = 0,$$

but,

$$\omega = \nabla \times v = \nabla \times \nabla^\perp \Psi = \Delta \Psi$$

thus,

$$\omega_t + \nabla^\perp \Psi \cdot \nabla \Delta \Psi - \nu \Delta \Delta \Psi = 0 \qquad (1.8)$$

Now, is possible to see that the equation (1.7) is analogy to the equation (1.8), considering stationary conditions ($\omega_t = 0$) and non viscous fluid ($\nu = 0$),therefore we can do the do a parallel between fluid and image, where

Fluids	Image
Fluid flow function Ψ	Image Intensity u
velocity $v = \nabla^\perp \Psi$	direction isolines of $u, \nabla^\perp u$
vorticity ω	smoothness $\omega = \Delta u$
viscosity ν	diffusivity ν

Thus, if we resolve a problem of NS, we are automatically resolving a problem of image inpainting. Moreover, numerical solutions of the Navier and Stockes problems are well known.

A important point to get in consideration is when and why use the diffusion term.

The diffusivity work like a stabilization, because without it, the resolution methods normally diverge, but using this term the solutions change. So, to minimize the error and to guaranty the convergence we can choose a expression like this, with k as parameter:

$$\nu(\|\nabla^\perp u\|) = \frac{1}{1 + \frac{\|\nabla^\perp u\|}{k}}$$

Thereby, when we have a high gradient of u, the diffusion is negligible in order to preserve the image's edge.

1.4.4 Fusion Method

After we do the Metal Artifact Reduction, in some cases, in exchange of remove the artifact, some pieces of the image are corrupted, pieces that are important to understand the image.

If these pieces were on the original image, a method called fusion based prior image can be use to recover these piece that was corrupted during the MAR.

This method is based on merge, in some way, the original image with the reconstruct image (pos-MAR) generating a new image called prior image. Subsequently, this image pass by another process of metal artifact reduction.

In this process, instead of interpolate directly the "sinogram", we subtract the "sinogram" of the original image by the "sinogram" of the prior image and then do the interpolation. After, the prior sinogram is added to the last result and is done filtered back projection to obtain the recovered image.

To merge the two images the equation (1.9) is used:

$$I_{prior}(i,j) = w(i,j) \cdot I_{ori}(i,j) + [1 - w(i,j)] \cdot I_{pos}, \qquad (1.9)$$

where $w(i,j)$ is calculated through:

$$w(i,j) = \frac{1}{1 + [\frac{D_{norm}(i,j)}{t}]^n}$$

$$D_{norm}(i,j) = \frac{D(i,j) - D_{min}}{D_{max} - D_{min}}$$

Where t and n are two parameters that assert how take a pixel from the pos-MAR image and from the original image. $D_{norm}(i,j)$ is the difference between these two images and D_{max} and D_{min} are the maximum and minimum value of D.

Chapter 2

Algorithm

2.1 Structure of a interpolation method

In this section we will see how was implemented the interpolation method. The steps for the implementation are:

1. Segmentation of metallic part on the corrupted image.

2. Radon transform of the corrupted image.

3. Identification of the inpainting domain based on the radon transform of metallic part identified

4. Inpainting of the domain using the interpolation technique.

5. Filtered back projection of the inpainted sinogram

6. Merge of the restored image with the segmented metallic part.

Except for the step 4, all of them are implemented in Matlab. The step 4 depend of the method, for the Linear interpolation we adopt only matlab, for the Interpolation of Bertalmio et al., we adopt Matlab and FreeFem++, to solve the partial differential equation. On the next part we will explain how each step is done.

See the figure (2.1) for a visual model of the schema.

2.2 Segmentation

The segmentation of metallic part on the corrupted image is done using a threshold. However, this process is not enough due to some false positive, so we apply a closing morphological operator eliminating these problems. The figure (2.2) show what happen on each step.
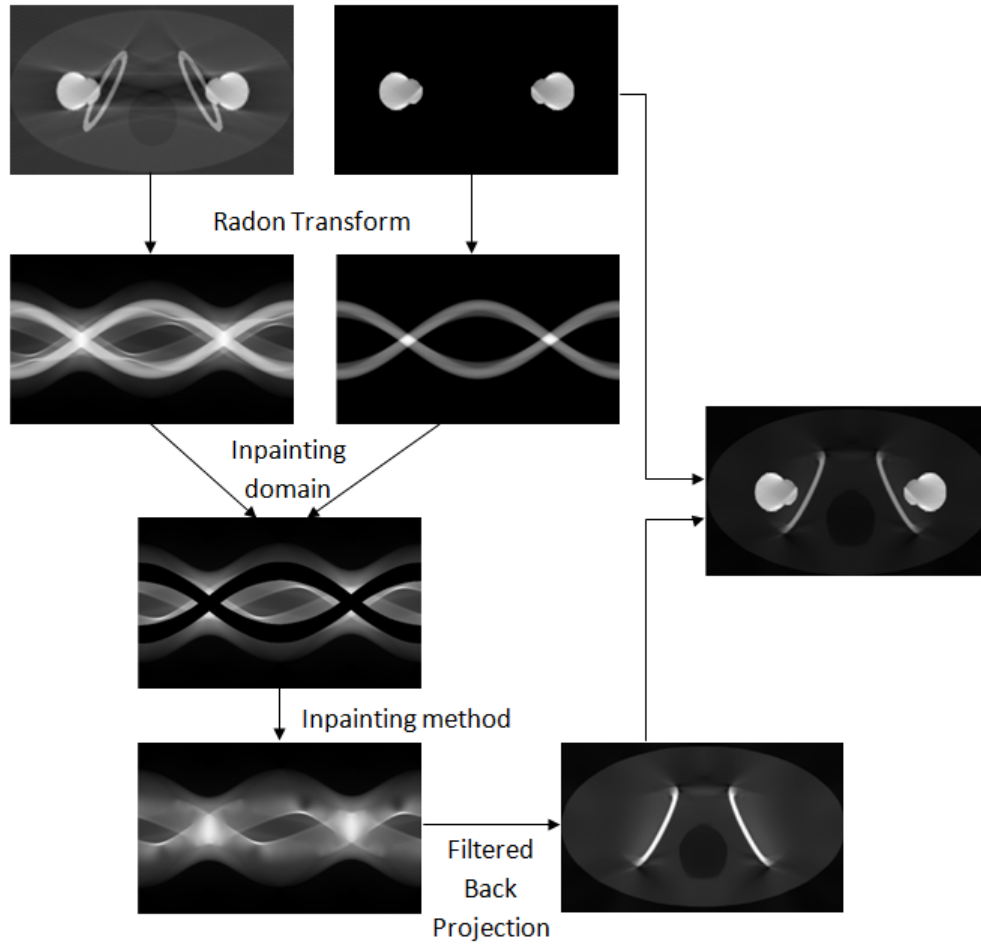
Figure 2.1: General Scheme

2.3 Radon Transform

In Matlab there is a function that execute the Radon transform of a image. To use it we pass as parameter the image and a vector with all the angles to calculate the projections.

2.4 Linear interpolating

The linear interpolating is done taking in account the vertical extreme of the each side of domain, so a linear function is traced between them, using the function interp1 provided by Matlab. It is worth mentioning that the interpolating is done one time for each value of 'x' coordinate of the sinogram, that represent a projection angle.

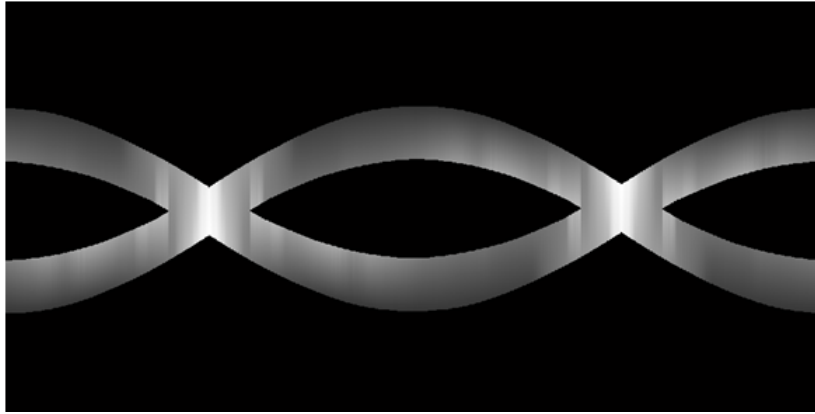Figure 2.2: Segmentation Step. image after the threshold(left), image after closing operator(right).

Figure 2.3: A linear interpolation, we can see a discontinuity on the 'x' coordinate, because the interpolation happens only on the 'y' coordinate

2.5   Bertalmio et al. interpolating

The method of Bertalmio consist in resolve two partial differential equation. This task is divided on two great step, divided the domain in a triangular grid and solve the PDE using finite element. To execute the triangulation we used the function DelaunayTri on Matlab, where each pixel represent a vertex of a triangle.

The function DelaunayTri request two thing: The points that will be the vertex of the triangles (In our case all the pixel inside the inpainting domain) and the constraints, i.e, the boundary of the domain. If we don't use any constraints, the grid will be convex hull of our domain.(2.4)

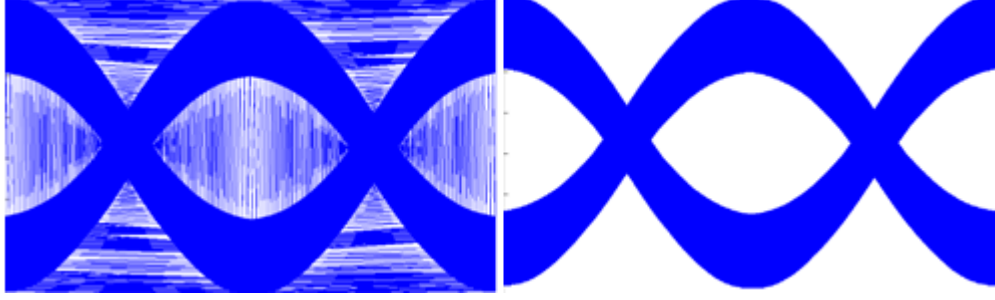To solve the PDE which the equation is described by (2.1) and (2.2) we used the software Freefem++.

Figure 2.4: The triangular grid without the constraints (left) and with constraints (right)

$$\begin{cases} -\nu\Delta v + v \cdot \nabla v + \nabla p = 0 & D \\ \nabla \cdot v = 0 & D \\ v(:,0) = v(:,2\pi) & D \\ v = \nabla^{\perp} u_{orig} & \partial D \setminus \{(x,\theta)|\theta = 0 \, or \, \theta = 2\pi\} \\ \nu = \frac{1}{1 + \frac{\|\nabla^{\perp} u\|}{k}} \end{cases} \qquad (2.1)$$

$$\begin{cases} \nabla^{\perp} u = v & D \\ u(:,0) = u(:,2\pi) & D \\ u = u_{orig} & \partial D \setminus \{(x,\theta)|\theta = 0 \, or \, \theta = 2\pi\} \end{cases} \qquad (2.2)$$

The numerical resolution is done using the Galerkin-finity element with the fixed point approximation for the non-linearity part. The dirichlet border conditions is done with the penalty method. On the equation(2.2) is applied a rotational operator. The weak formulations is expressed by:

$$\begin{cases} a(v^k, w) + c(v^{k-1}, v^k, w) + b(w, p^k) = F(w) & \forall w \in V \\ b(v^k, q) = 0 & \forall q \in Q \end{cases} \qquad (2.3)$$

$$\begin{cases} a_2(u, \psi) = F_2(\psi) & \forall \psi \in R \end{cases} \qquad (2.4)$$

where

$V = V(D) = \{w(x',\theta)|w = \Sigma_n w_n \alpha_n(x',\theta), w_n \in \mathbb{R}, (x',\theta) \in D, w(:,0) = w(:,2\pi)\}$

$Q = Q(D) = \{q(x',\theta)|q = \Sigma_n q_n \beta_n(x',\theta), q_n \in \mathbb{R}, (x',\theta) \in D\}$

$R = R(D) = \{r(x',\theta)|w = \Sigma_n r_n \gamma_n(x',\theta), r_n \in \mathbb{R}, (x',\theta) \in D, r(:,0) = r(:,2\pi)\}$

$$a(v,w) = \nu \int_D \nabla v \nabla w + \lambda \int_{\partial D'} vw$$

$$c(u,v,w) = \int_D (u \cdot \nabla) v \cdot w$$

$$b(w,q) = - \int_D q(\nabla \cdots w)$$

$$F(w) = \lambda \int_{\partial D'} v_{orig} w$$

$$v_{orig} = \nabla^\perp u_{orig}$$

$$a_2(u,\psi) = \int_D \nabla u \nabla psi + \lambda \int_{\partial D'} u\psi$$

$$F_2(\psi) = - \int_D (\nabla \times v)\psi + \lambda \int_{\partial D'} u_{orig}\psi$$

$$\partial D' = \partial D \setminus \{(x,\theta) | \theta = 0 \, or \, \theta = 2\pi\}$$

The problems (2.3) and (2.4) are solved using finite element in P1b, for $\alpha_n(V_h)$, P1, for $\beta_n(Q_h)$ and P2, for $\gamma_n(R_h)$.

Because of the non linearity of the problem (2.3),it need be solved iteratively until reach a stopping criterion. The criterion are:

- $\frac{\|v_k - v_{k-1}\|_{H^1}}{\|v_0\|_{H^1}} < \varepsilon$

- Maximum number of iteration

- $\frac{\|v_k - v_{k-1}\|_{H^1}}{\|v_0\|_{H^1}} > \beta$ (In this case the solution is diverging, so we stop the algorithm)

Each iteration use the Schur complement to create a linear system that is solved through GMRES. Additionally, a matrix need to be passed as precondition to accelerate the resolution of the linear system. We have two candidates:

- The matrix Mp^{-1} formed by the $m(p,q) = \int_D pq$ where $p,q \in Q_h$

- The diagonal matrix M^{-1} formed by the diagonal elements of Mp

After all, the problem (2.4) can be solved direct.

Both problems have a Dirichlet conditions, these conditions is what associate the image inpainting with a fluid dynamics problem, thus is a high important part. The problem (2.2) have as 'entry' the pixel intensity of the image that is taken direct.

However, the problem (2.1) have as 'entry' a stream line of the pixel intensity, to calculate it we used finite different method of first order additionally a medium filter. The medium filter is necessary to reduce the noise and preventing it to alter the image inpainting.

2.6 Inverting the sinogram

To invert the sinogram we do the filtered back projection using a function called 'iradon' provided by the Matlab. Subsequently we apply a edge-preserving blur filter.

This filter is a medium filter, however instead of use all nearest pixel to calculate the mean, use only the nearest pixel with the intensity is similar, thereby, preserving the edge. Mathematically can be write like this:

$$M(i,j) = \frac{\Sigma_{p=-v}^{p=v}\Sigma_{q=-v}^{q=v}B(i+p,q+q)}{N}$$

$$B(i+p,j+q) = \begin{cases} 0 & |b(i+p,j+q) - b(i,j)| > T \\ b(i+p,j+q) & |b(i+p,j+q) - b(i,j)| < T \end{cases}$$

where, T is a threshold, v a window, b the pixel intensity.

Lastly we add the segmented metal part to the inverted image to obtain the restored image.

Chapter 3

Result

The first analysis that we will do is a comparison between the liner method and the Bertalmio et al.

To do this comparison we use the image (3.1).

Figure 3.1: Real Hip Phantom

The image (3.1) represent a hip phantom with bilateral prostheses. However, this is the real image, when we do the tomography the metallic prostheses hinder the process, so the acquired image is different. So we need to generate it.

3.1 Generating the artifacts

To generate the corrupted image we interpret this image as the tomography machine do. So the first step is to swap the intensity of a pixel by the value that represent the electrical density. The next step is to do the radon transform of the "electrical density image" and them to select the points(pixel) with the intensity is greater than a determined value and replace these values to the threshold. This operation is done because the machine isn't able to measure the x-ray's intensity when there is a high absorption. So it interpret these measure that is meaningless as the maximum

absorption that the machine is able to recognize.

On the last step we do the filtered back projection to obtain the corrupted image which we apply a median filter. The figure (3.2) illustrate the process.
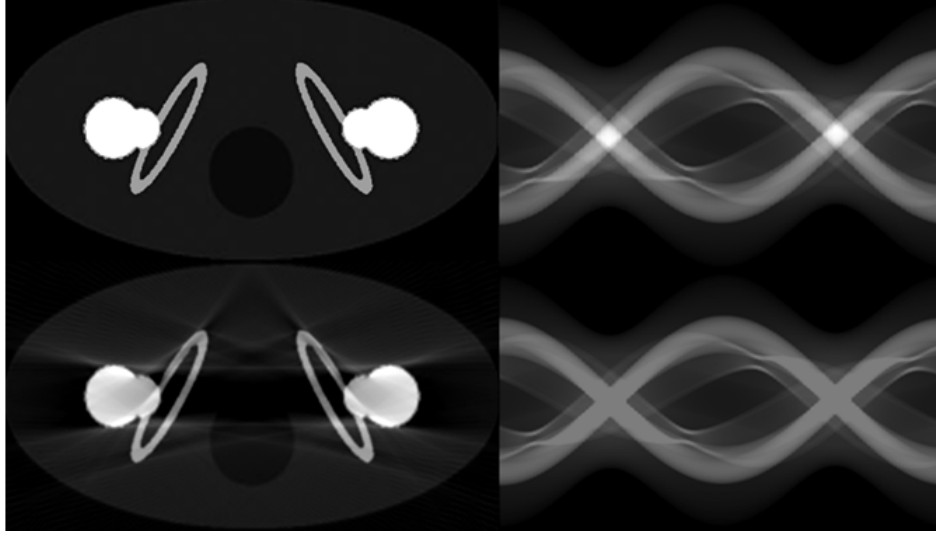

Figure 3.2: Upper left: Original Phantom; Upper right: Sinogram of the original phantom; Bottom Left: Restored corrupted sinogram; Bottom Right: Corrupted sinogram derived from the upper bound of the original sinogram.

3.2 Evaluation Procedure

The comparison is realized in quantitative and qualitative way. The qualitative part is based on the visual analyses of the image and its sinogram.

The quantitative is composed by five index that determine how much similar are two images and the analysis of the intensity of the pixel along a line in the figure.

The index used are:

- MSE: Mean Squared Error

$$MSE = E[(I_{cor} - I_{ref})^2]$$

Where I represents the pixel intensity.

- PSNR: Peak-Signal-to-Noise Ratio

$$PSNR = 10 \log_{10} \left(\frac{max^2(I_{ref})}{MSE} \right)$$

Bigger is this value, more similar are the images

- NCC: Normalized Correlation Coefficient

$$NCC = E\left[\frac{(I_{cor} - \mu_{cor})(I_{ref} - \mu_{ref})}{\sigma_{cor}\sigma_{ref}}\right]$$

Where μ and σ are the mean and standard derivation of the image. Nearest one, more similar are them

- MSSIM: Mean Structure Similarity Index

$$MSSIM = E[SSIM]$$

$$SSIM = \frac{(2\mu_{ref}\mu_{cor} + c_1)(2\sigma_{ref}\sigma_{cor} + c_2)}{(\mu_{ref}^2 + \mu_{cor}^2 + c_1)(\sigma_{ref}^2 + \sigma_{cor}^2 + c_2)}$$

Where μ and σ are the mean and standard derivation of a window, and c_1 and c_2 are two constants. This index show the similarity with respect to the human vision. Nearest one, better.

- FSIM: Feature Similarity Index

These five index, are calculated in 2 different regions which can be seen in the figure (3.3). While, the line used to compare the intensity can be seen in the figure (3.4);
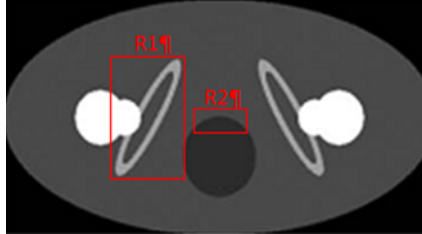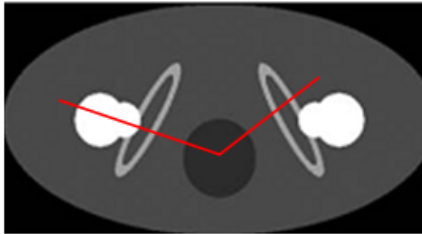

Figure 3.3: Regions to calculate the index

Figure 3.4: Pixel Intensity Line

3.3 Bertalmio at el.

Initially we well do a analysis of the method of Bertalmio at el. and how it change with the tuning parameters K and the dilation of the inpainting domain:
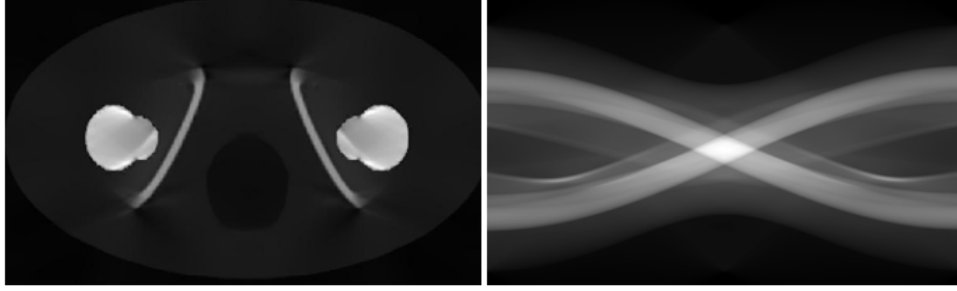

Figure 3.5: A tunned Bertalmio et al interpolation. Dilatation = 8 and k=10

	Region 1					Region 2				
	MSE	PSNR	CC	MSSIM	fsim	MSE	PSNR	CC	MSSIM	fsim
Artifact	4.262	17.567	0.920	0.338	0.974	1.121	3.349	0.159	0.000	0.936
Bertalmio	6.360	15.828	0.882	0.400	0.936	0.024	20.020	0.959	0.574	0.981

The method of Bertamio is capable to retrieve the information in the middle of the image, represented by the region two, but appear a new artifact on the region one. In the graph (3.6) is easy to see that the method of Bertalmio ignore the existence of the bone nearest of the metal. However, it 'fix' the problem that appeared between the two implants, in the artifact image we have negative values on this region, while on the Bertalmio image the intensity is almost equal to the reference.
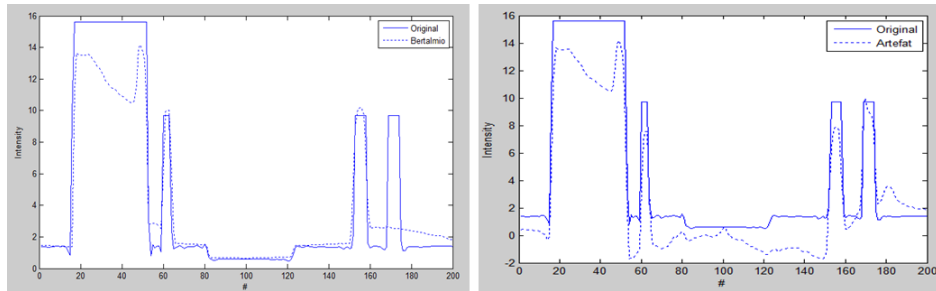

Figure 3.6: Line comparison between restored(Bertalmio) image (left) and corrupted image(right).

3.3.1 Parameter Dil

The parameter Dilatation (Dil) is difficult to tuning, this happens because each image need a different one and it don't have a well defined tendency. The way that we use to chose this parameters is trial and error, obvious this method is very inefficient due to the high execution time of each try.
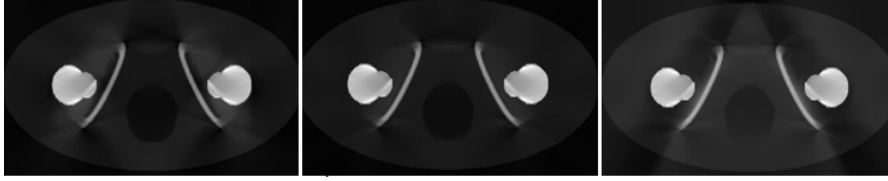

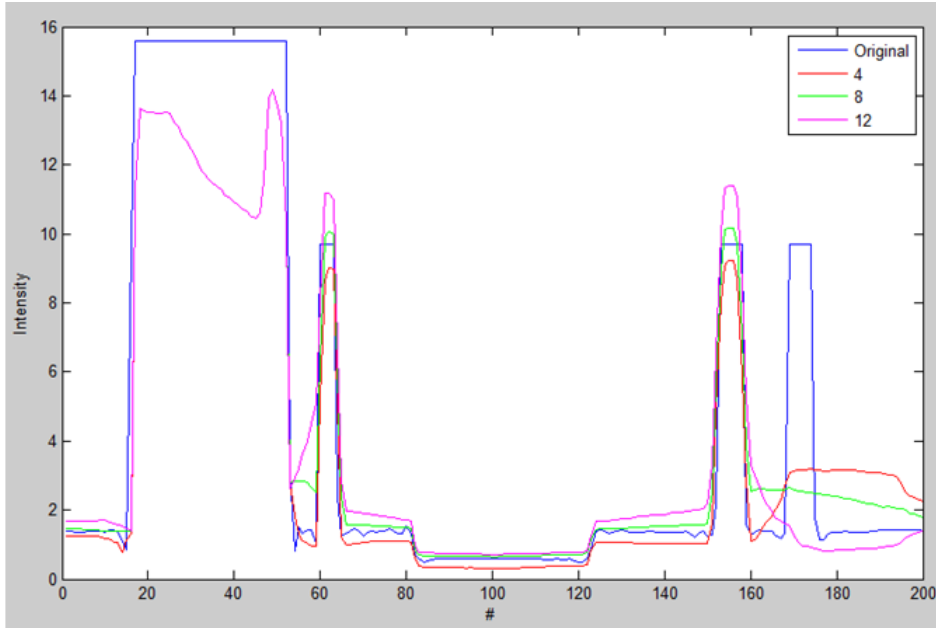Figure 3.7: Dil comparison. Dil=4(left) Dil=8(middle) Dil=12(right)

Figure 3.8: Dilatation line comparison

The graph (3.8) show the reason for the difficult to set the parameter, if the parameters is smaller or greater than a optimal is not possible judge if a better solution is reach increasing or decreasing it. The general rule is take the the shortest possible one ,in such way, the majority part of the artifact are surrounded.

25

3.3.2   Parameter K

The parameter of stabilization K has a important role of guarantee the convergence. Despite, in theory, a larger parameter K increase the error, it didn't happened in our case, since the blur edge filter make up the error. Furthermore, K interferes direct on the time of convergence of the method, as shown on the graph
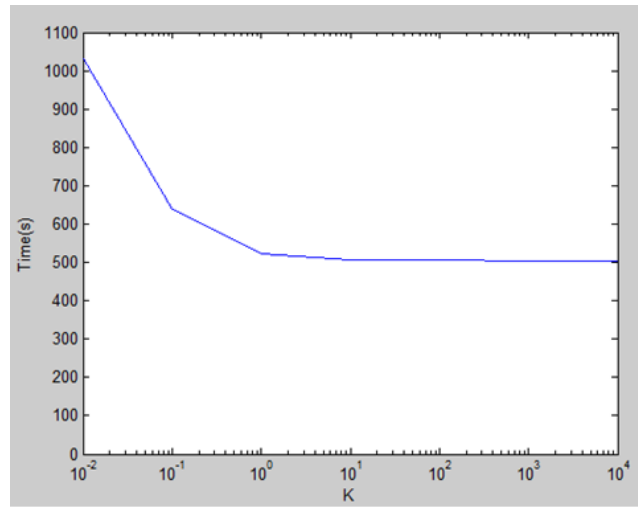

Figure 3.9: Convergence time x K
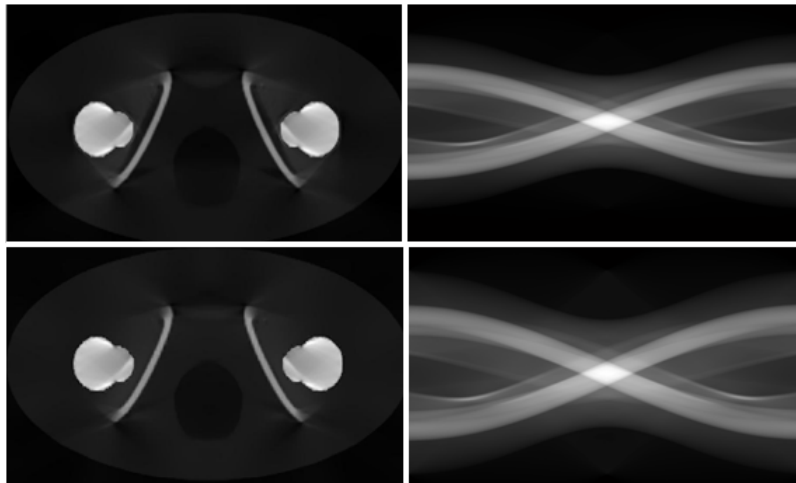
3.3.3   Linear x Bertalmio

Figure 3.10: Upper side: Linear restoration. Botton side: Bertalmio et al restoration

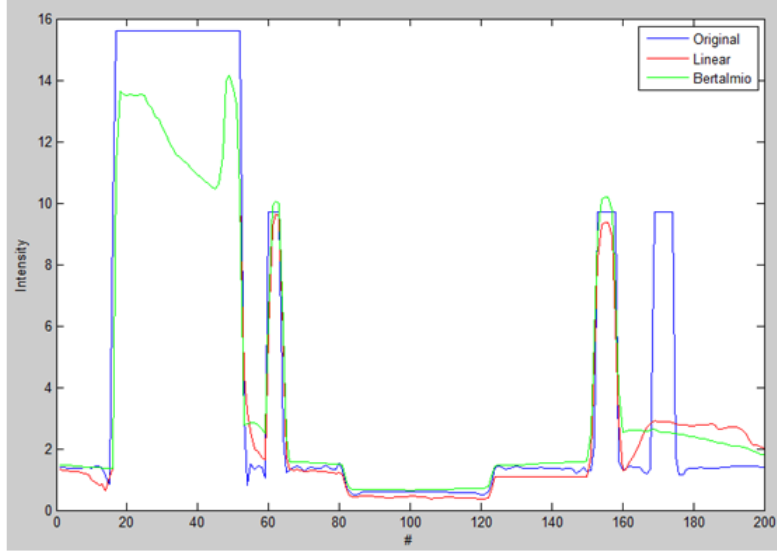|	Region 1					Region 2				
	MSE	PSNR	CC	MSSIM	fsim	MSE	PSNR	CC	MSSIM	fsim
Artifact	4.262	17.567	0.920	0.338	0.974	1.121	3.349	0.159	0.000	0.936
Linear	6.047	16.047	0.894	0.381	0.933	0.065	15.691	0.979	0.631	0.981
Bertalmio	6.360	15.828	0.882	0.400	0.936	0.024	20.020	0.959	0.574	0.981

Figure 3.11: Line comparison between the Linear and Bertalmio et Al interpolation

Comparing the two methods we can arrive a two conclusions: On the phantom hip, the two methods is almost equivalent, they have the same problem on the bone near to the metal implant and the remainder part is very similar to the original image. The linear method is slight better considering the the image edges (see the pixel 60 and 160 on graph (3.11)).

3.4 Fusion

The second analysis is regard to the fusion method. On this method there are two restoration process, so we will use all possible combination and compare then. The combination are Linear/Linear, Linear/Bertalmio, Bertalmio/Linear and Bertalmio, Bertalmio. The fusion method has two parameters, n and t. We test how them change the restoration only for the case Linear/Linear, after we extrapolate the better parameters for the other cases.

27

3.4.1 Parameter t

The parameter t is the most important to set accordingly, because if it's low the fusion method don't work, and if is high the artifact is not removed.
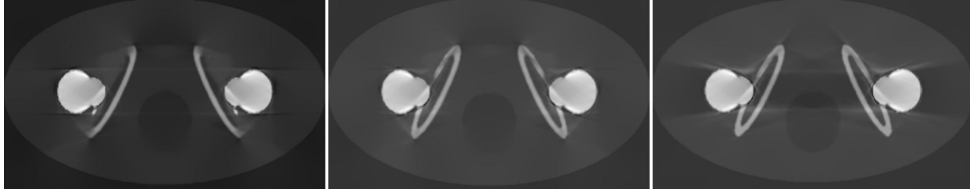

Figure 3.12: t comparison. t=0.15(left) t=0.45(middle) t=0.75(right)

3.4.2 Parameter n

The parameter n is relevant, however is not fundamental set it to the right value. The prove show us that the best parameter depend of the region, additionally the difference are negligible , so we choose a intermediary parameter.
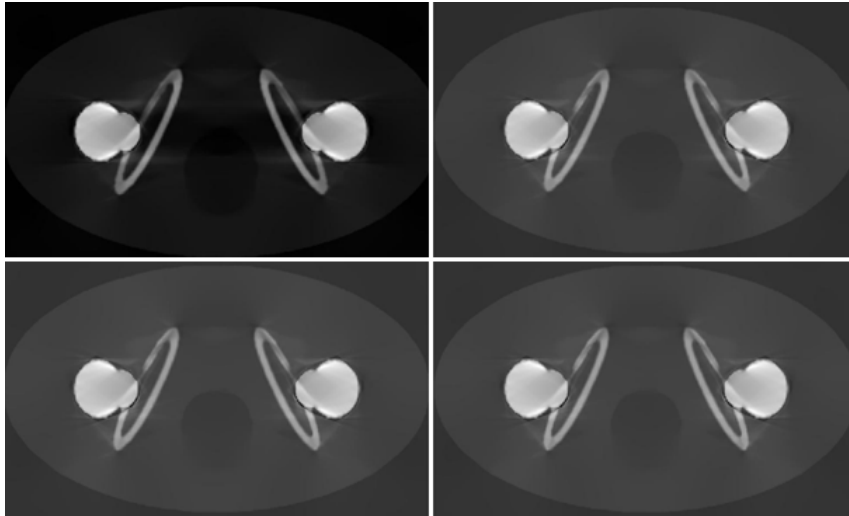

Figure 3.13: n comparison. n=1(top/left) n=5(top/right) n=10(down/left) n=20(down/right)

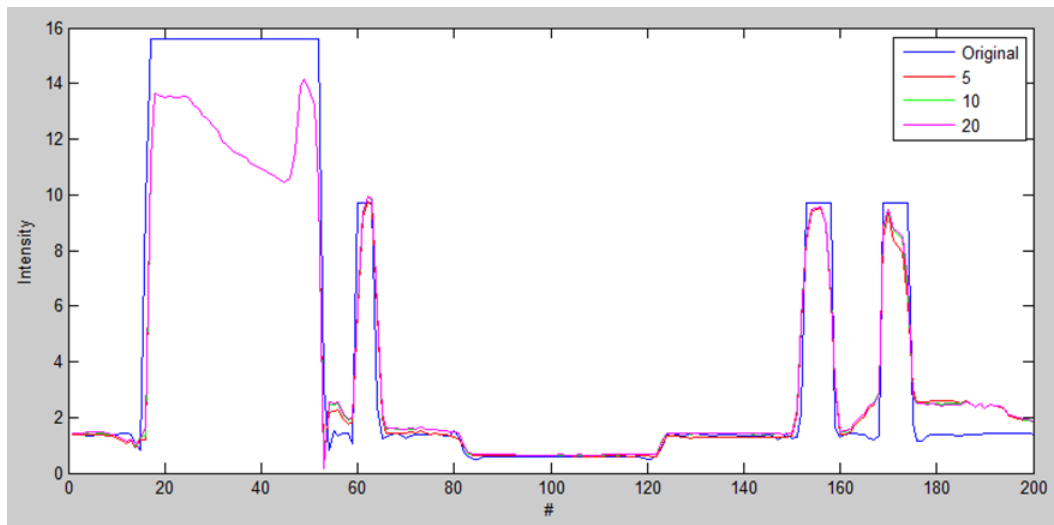|	Region 1					Region 2				
	MSE	PSNR	CC	MSSIM	fsim	MSE	PSNR	CC	MSSIM	fsim
Artifact	4.262	17.567	0.920	0.338	0.974	1.121	3.349	0.159	0.000	0.936
1	4.382	17.446	0.930	0.396	0.965	0.482	7.017	0.816	0.135	0.963
5	4.426	17.403	0.924	0.411	0.964	0.025	19.879	0.917	0.418	0.962
10	4.307	17.520	0.926	0.436	0.965	0.035	18.456	0.915	0.418	0.961
20	4.380	17.448	0.924	0.426	0.964	0.038	18.103	0.900	0.388	0.959

Figure 3.14: Line comparison for diferent n parameters
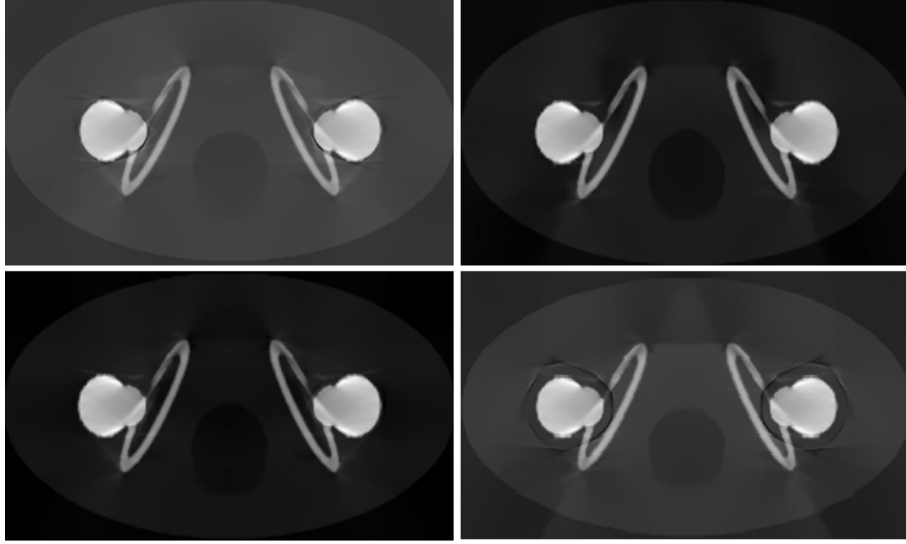
3.4.3 Combination Method

Figure 3.15: Method comparison. Linear/Linear(top/left) Bertalmio/Bertalmio(top/right) Linear/Bertalmio(down/left) Bertalmio/Linear(down/right)

Qualitatively we can disregard the combination Bertalmio/Lin due to the clear additional artifact. The combination Bertalmio/ Bertalmio isn't acceptable as well, because of the high time consummation of the method.

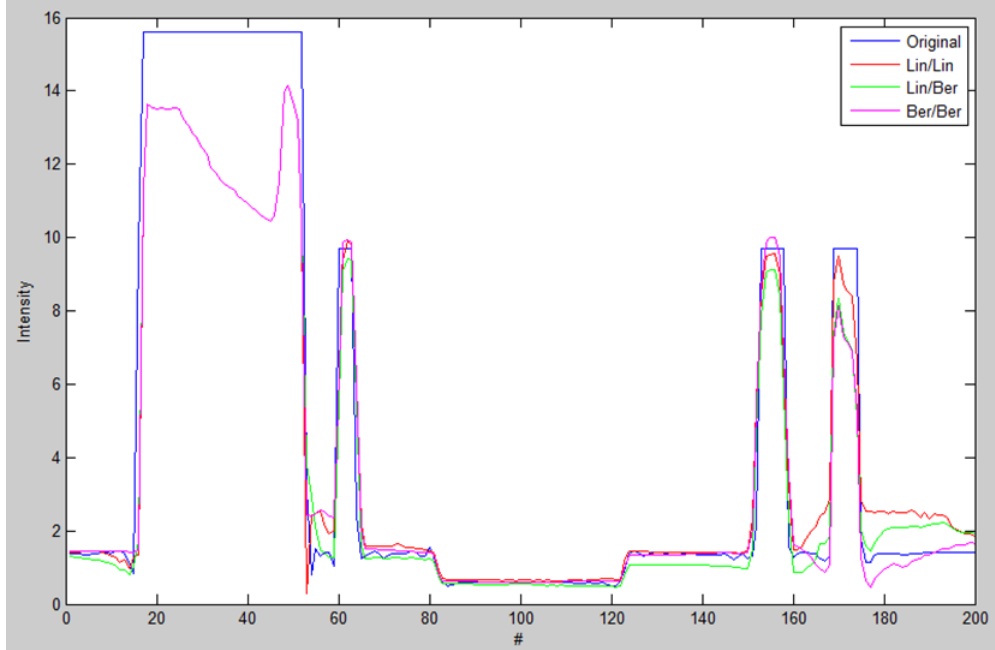|	Region 1					Region 2				
	MSE	PSNR	CC	MSSIM	fsim	MSE	PSNR	CC	MSSIM	fsim
Artifact	4.262	17.567	0.920	0.338	0.974	1.121	3.349	0.159	0.000	0.936
Lin/Lin	4.380	17.448	0.924	0.426	0.964	0.038	18.103	0.900	0.388	0.959
Ber/Ber	3.866	17.989	0.935	0.512	0.970	0.009	24.236	0.970	0.643	0.982
Lin/Ber	3.768	18.102	0.943	0.498	0.969	0.049	16.925	0.981	0.681	0.984
Ber/Lin	4.315	17.513	0.918	0.397	0.962	0.397	7.861	0.886	0.272	0.962

Figure 3.16: Line comparison for different methods

The results show us that there isn't a method that surpass the other. Depending of the regions a method is better or not. For instance, the method Linear/Bertalmio have the lowest MSE, however between the pixel 120 and 150 the error is very high.

3.5   Final analysis

The phantom hip was a good image to test the method. Using it we arrived to two conclusions:

The method of Bertalmio is not a good method when the inpainting domain is large. It is not surprising because if we have less information, the estimate will be courser, thus don't have much sense use a method that require more time to execute a finer estimate.

Differently, the fusion method performed very well and the goal of retrieve the loss of information was achieved. However, some artifact arise. It can be a problem or not, all depend of which part the doctor want to see to do the diagnostic.

Bibliography

[1] Elena Faggiano, Tommaso Lorenzi and Alfio Quarteroni (2014): Metal artefact reduction in computed tomography images by a fourth-order total variation flow, Computer Methods in Biomechanics and Biomedical Engineering: Imaging & Visualization, DOI: 10.1080/21681163.2014.940629

[2] M. Haile , Restauro di immagini tomografiche mediche tramite l'uso di metodi di image inpainting, 2013.

[3] Jun Wang, Shijie Wang, Yang Chen, Jiasong Wu, Jean-Louis Coatrieux, and Limin Luo "Metal artifact reduction in CT using fusion based prior image",Am. Assoc. Phys. Med. 2013.

[4] P. Kuchment. The Radon Transform and Medical Imaging. Philadelph, Siam, 2014.

[5] A. Quarteroni. Modellistica numerica per problemi differenziali,3a edizione, Milano, Spinger, 2006.